

Single-Phase Direct AC-AC Boost Converter

Mihai LUCANU, Ovidiu URSARU, Cristian AGHION, Nicolae LUCANU
Gheorghe Asachi Technical University of Iasi, Faculty of Electronics, Telecommunications and
Information Technology, Blvd. Carol I, No. 11, 700506, Iasi, Romania
aghion@etti.tuiasi.ro

Abstract—The paper presents a single-phase direct AC-AC boost converter. The circuit of the converter is simple and it has good performances, irrespective of the load nature. The adequate functioning and high performance of the circuit (the efficiency and waveform of the absorbed input current) were tested both by simulation and experimentally.

Index Terms—choppers, circuit simulation, power conversion.

I. INTRODUCTION

AC-AC converters are currently used in numerous fields, such as AC motor drives, adjustable AC sources, electric transformers, output voltage waveform restorers etc. These converters successfully replace alternative voltage variators using SCRs or TRIACs. Since operation frequencies are higher (over 20 KHz), there is no noise, filters are smaller in size, the efficiency is higher and the current taken from the grid is nearly sinusoidal.

The first AC-AC converters (AC choppers) subject to analysis were buck converters [1]. References [2]-[4] present improved PWM techniques, which increase the power factor and eliminate certain harmonics. In [5], an IGBT chopper with a 5kHz frequency was analyzed by simulation. Reference [6] presents a three-phase AC-AC converter with nine IGBTs and [7] suggests a method for evaluating three-phase AC-AC converters. In [8] and [9], the proposed AC choppers are characterized by improved switching and high efficiency, however the circuits are quite complex. References [10] and [11] present AC choppers with three-level converters and topologies using commercial power modules. A high-performance single-phase AC converter involving two inductances and four IGBTs is presented in [12].

The paper presents a single-phase direct AC-AC boost converter using only two IGBTs and one inductance (except for the grid filter). The functioning equations presented are used for design purposes. The converter can supply a bidirectional power flow. The functioning frequency is 20 kHz, the efficiency is high and the input current is nearly sinusoidal. This frequency was chosen since it goes beyond the range of acoustic frequencies perceived by the human ear and in order to be able to use IGBT's. Certainly, a higher switching frequency of the converter will determine lower values for the inductances and capacitors in the circuit presented. The simulation allowed us to test the adequate functioning and to deduce the control characteristic of the AC-AC boost converter. The circuit functions adequately both for resistive and inductive loads.

One of our purposes was the correction of the input current waveform. Given that the supply voltage is sinusoidal, the most favorable sampling is uniform sampling, which we used in the paper, because the average values of the voltage (therefore of the current) for various sampling periods remain sinusoidal, which leads to the minimization of the harmonics for the current supplied by the power source. The circuit can be used when it is necessary to increase the load voltage, especially for voltage conversion from 110V to 220V, with some control adjustments when the input voltage values vary in the range $\pm 10\%$.

II. CIRCUIT ANALYSIS

Figure 1 presents the circuit of the single-phase AC-AC boost converter comprising the L_f and C_f filter, the L_l inductor, the C capacitor connected in parallel with the load impedance and two AC switches, each made up of four diodes and one IGBT. The load impedance Z has the voltage v_o and the current i_o . In fact, without the grid filter, the circuit is a classic boost converter, except that the transistor and the diode are replaced by two bidirectional current switches.

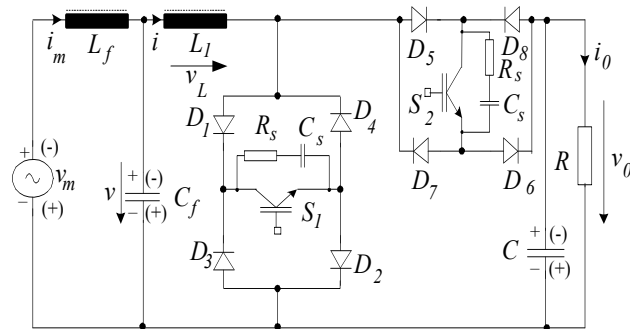


Figure 1. Single-Phase Direct AC-AC Boost Converter

Figure 2 presents the waveform of the v voltage and the generation of the control signals of IGBTs S_1 and S_2 . If the current through the L inductor is $i > 0$ for time intervals $[0, DT]$, it will flow through L_l , D_1 , S_1 , D_2 , and for time intervals $[DT, T]$ it will flow through L_l , D_5 , S_2 , D_6 and the L , R load. If $i < 0$ for time intervals $[0, DT]$, the i current will flow through D_3 , S_1 , D_4 , L_l and for time intervals $[DT, T]$, it will flow through the load circuit D_8 , S_2 , D_7 , L_l . The supply of the R , L load is insured by capacitor C .

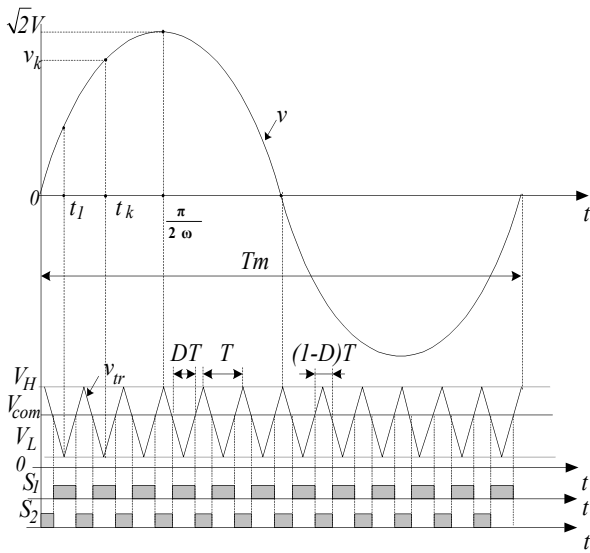


Figure 2. The waveform of the v voltage and the generation of the control signal for IGBTs

PWM control is used, where the switching durations of the two switches are constant for all T switching periods, similarly to the DC converters, and $f = 1/T$ is the switching frequency. The load impedance is:

$$Z = \sqrt{R^2 + (\omega L)^2}, \quad \omega = 2\pi f_m, \quad f_m = \frac{1}{T_m} \quad (1)$$

The equations characterizing the functioning of the converter are deduced under the following simplifying hypotheses: the passive components are ideal, the power devices are ideal switches, the v voltage on the C_f capacitor and v_0 voltage on the load are sinusoidal and remain constant for a T period, and the load is purely resistive ($L=0$). For an inductive load, the equations do not change significantly.

$$\begin{cases} v = \sqrt{2} \cdot V \cdot \sin \omega t \\ v_k = \sqrt{2} \cdot V \cdot \sin \omega t_k = \text{const}, \quad t_k = (k-1)T + \frac{T}{2} \\ v_{0k} = \sqrt{2} \cdot V_0 \cdot \sin \omega t_k = \text{const}. \end{cases} \quad (2)$$

For the interval $[0, DT]$, when S_1 is ON and S_2 is OFF:

$$\begin{cases} L_1 \frac{di_{1k}}{dt} = v_k \\ i_k = I_{km} + \frac{v_k}{L_1} t \\ v_L = v_k \end{cases} \quad (3)$$

If we apply the i_{1k} equation for $t=DT$, we obtain:

$$\begin{cases} i_k = I_{km} = I_{km} + \frac{v_k}{L_1} DT \\ \Delta i_k = I_{km} - I_{km} = \frac{Dv_k}{L_1 f} \end{cases} \quad (4)$$

For the interval $[DT, T]$, when S_1 is OFF and S_2 is ON:

$$\begin{cases} v'_L = -(v_{ok} - v_k) \\ i'_k = I_{KM} - \frac{v_{ok} - v_k}{L_1} t', \quad t' \in [0, (1-D)T] \end{cases} \quad (5)$$

Since it is a boost converter, the control characteristic corresponding to a T switching period can be approximated by the equation:

$$v_{0k} = \frac{v_k}{1-D} \quad (6)$$

and the average value of the i current for a T period is

$$I_K = \frac{v_k}{(1-D)^2 R} \quad (7)$$

Similarly, we obtain the following average values of the currents for the bidirectional switches, corresponding to a T period:

$$\begin{cases} I_{S1K} = \frac{Dv_k}{(1-D)^2 R} \\ I_{S2K} = \frac{v_k}{(1-D)R} \end{cases} \quad (8)$$

and the following values for the maximum repetitive currents

$$I_{S1KM} = I_{S2KM} = I_K + \frac{\Delta i_k}{2} = \frac{v_k}{(1-D)^2 R} + \frac{Dv_k}{2L_1 f} \quad (9)$$

The maximum voltages collector-emitter for the two IGBTs are:

$$V_{S1KM} = V_{S2KM} = v_{0k} = \frac{v_k}{1-D} \quad (10)$$

Taking into account the fact that v_k voltages have a sinusoidal variation, these are the final current and voltage requirements. The average current through the S_1 switch is:

$$I_{S1avr} = \frac{D}{(1-D)^2} \frac{2\sqrt{2}V}{\pi R} \quad (11)$$

$$I_{S2avr} = \frac{1}{1-D} \frac{2\sqrt{2}V}{\pi R} \quad (12)$$

and the maximum repetitive currents are:

$$I_{S1M} = I_{S2M} = \frac{\sqrt{2}V}{(1-D)^2 R} + \frac{D\sqrt{2}V}{2L_1 f} \quad (13)$$

The voltage stress of the IGBTs is:

$$V_{S1M} = V_{S2M} = \frac{\sqrt{2}V}{1-D} \quad (14)$$

The normalized current ripple results from equations (4) and (7)

$$\frac{\Delta i_k}{I_k} = \frac{D(1-D)^2 R}{L_1 f} \quad (15)$$

This equation is used in the design process for the calculation of the L_1 inductance.

The normalized ripple of the output voltage can be calculated with the equation:

$$\frac{\Delta v_0}{v_0} = \frac{D}{RCf} \quad (16)$$

This equation lies at the basis of the calculation of the C capacity connected in parallel with the load.

The calculation of the filter $L_f C_f$ components [13] –[17] requires the following data:

- Line frequency f_{Line}
- Minimal RMS voltage V_{min}
- Maximum RMS load current I_{max}
- Lowest switching frequency f_{swmin}

$$Z_D = \frac{V_{min}}{I_{max}} \quad (17)$$

The filter cutoff frequency f_{cut} is determined from the attenuation needed at the carrier frequency (plus a margin of 6 ... 10dB), while at the same time providing minimal attenuation at the line frequency.

$$f_{cut} > 10 f_{Line} \quad (18)$$

The L_f and C_f values of the filter are calculated as follows:

$$L_f = \frac{Z_D}{2\pi f_{cut}}, C_f = \frac{1}{2\pi f_{cut} Z_D} \quad (19)$$

III. SIMULATION RESULTS AND EXPERIMENTAL RESULTS

The adequate functioning of the circuit was tested by simulation and experimental prototype. The load used in the simulations and in the prototype is the same - a resistive load: $R=390 \text{ ohm}$;

The components of the simulated circuit have the following values: the grid filter is made up of $L_f=13\text{mH}$, $C_f=6\mu\text{F}$, the boost inductance is $L_l=5 \text{ mH}$, and $R=390\Omega$ for load. The amplitude of the grid voltage is 155V and the switching frequency is $f=20\text{KHz}$.

The simulations took into account the following values of the duty cycle: $D=0.4, 0.48$, and 0.56 . The paper presents only some of the waveforms obtained, namely the most representative ones. Thus, Figure 3 shows the waveforms of the v_m grid voltage and of the v_0 load voltage, as well as the waveforms of the i_m current supplied by the grid and the i_0 load current for $D=0.4$.

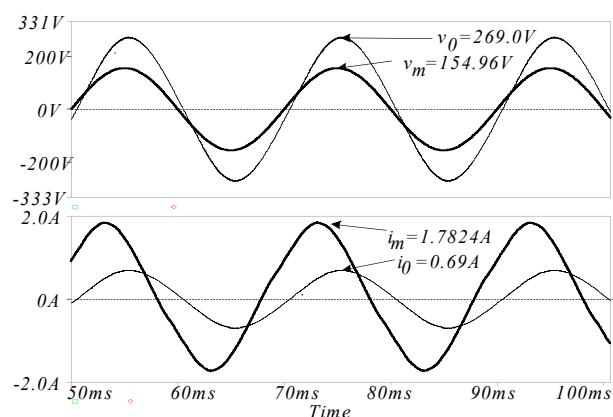


Figure 3. Waveforms of the v_m voltage, v_0 voltage, i_m current and i_0 current, for $D=0.4$

Figure 4 presents the same waveforms for $D=0.48$.

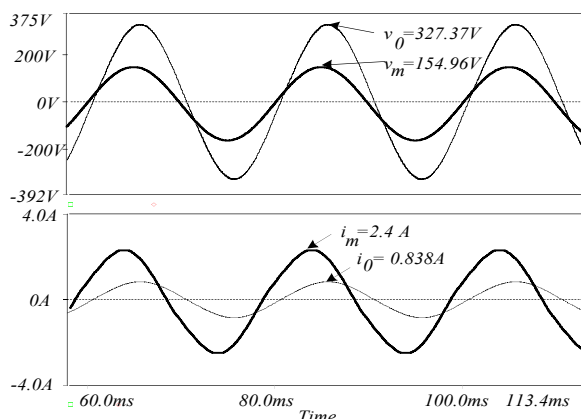


Figure 4. Waveforms of the v_m voltage, v_0 voltage, i_m current and i_0 current, for $D=0.48$

Figure 5 presents the same waveforms for $D=0.56$. The waveforms of the load voltage and current are nearly sinusoidal.

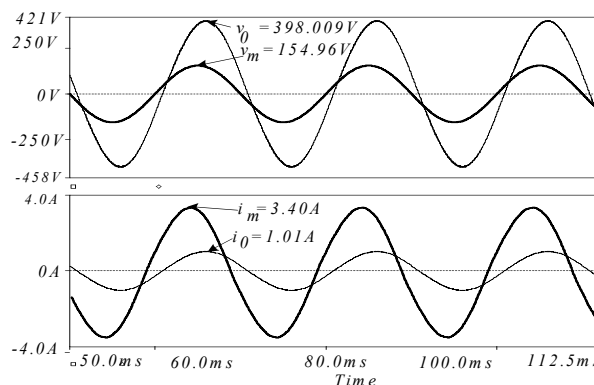


Figure 5. Waveforms of the v_m voltage, v_0 voltage, i_m current and i_0 current, for $D=0.56$

The laboratory prototype presented in Figure 6 was built and tested with the following parameters: input voltage $V_m = 110 \text{ V}$ and $f_m = 50\text{Hz}$. The components of the power supply filter are: $L_f=13\text{mH}$, $C_f=6\mu\text{F}$ and the switching frequency is $f=20 \text{ kHz}$.

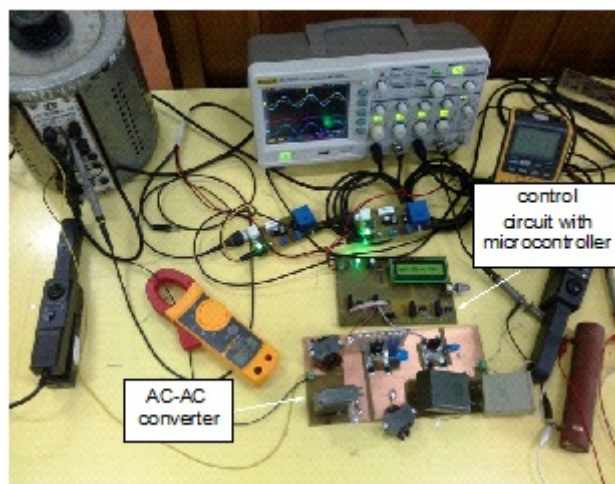


Figure 6. Experimental setup

The software was designed to be implemented on the PIC16F684 microcontroller, made by the MICROCHIP Company. It was chosen because it is cheap, easy to program and use. Figure 7 presents the flowchart of the software routine written in C programming language [18] for the PIC16F684 microcontroller, which works at 8MHz.

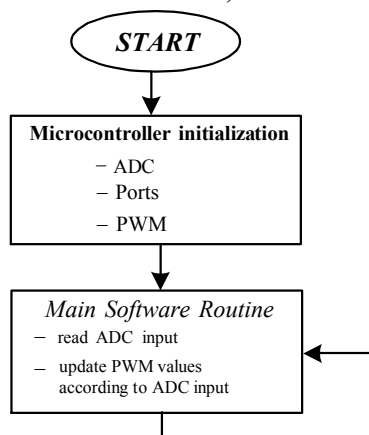


Figure 7. Flowchart of the software implemented on the microcontroller

At the beginning, the program variables are initialized, as well as some internal blocks of the microcontroller (ADC: Analog to Digital Converter, Ports: Input/Outputs Ports, PWM: Pulse Width Modulation). The program implemented on the microcontroller is aimed at obtaining two 20KHz PWM signals, which are complementary to each other, at the output pins P1A (pin 5) and P1B (pin 6) with no dead-time [19]. Since the experimental part was designed with the purpose of proving the concept of the power circuit, we chose the direct method of changing the duty cycle in accordance with the readings of an analogical voltage at pin AN2 (pin 11), where a potentiometer was installed. Depending on the analogical voltage read at this pin, the duty-cycle of the PWM signals from pins P1A and P1B is modified in order to get different PWM values necessary for testing the power circuit [20].

Using the microcontroller for the sole purpose of obtaining two PWM signals (with no dead-time) with fixed duty-cycle values is a rather complicated method; for the sake of simplicity, we could use a common oscillator with two complementary outputs. Nevertheless, we should mention that when we need closed-loop functioning in order to maintain constant the output voltage, the use of the microcontroller is an advantage.

The PWM signals generated by the microcontroller are applied to the two transistors S_1 and S_2 in Figure 1, by means of two HCPL3180 optocouplers. They are meant to separate the power circuit from the control circuit, insuring thus the galvanic isolation between them as a safety measure in case of malfunction.

As presented in Figure 6, the practical circuit is made up of two boards; one of them includes the microcontroller, the LCD, the drivers and the low-voltage supply circuit, and the other one contains the power circuit analyzed, whose schematic is presented in Figure 1.

Figure 8(a) shows the waveforms of the v_o voltage and of the v_m voltage and Figure 8(b) shows the waveforms of the i_o current and of the i_m current for a duty factor $D=0.4$.

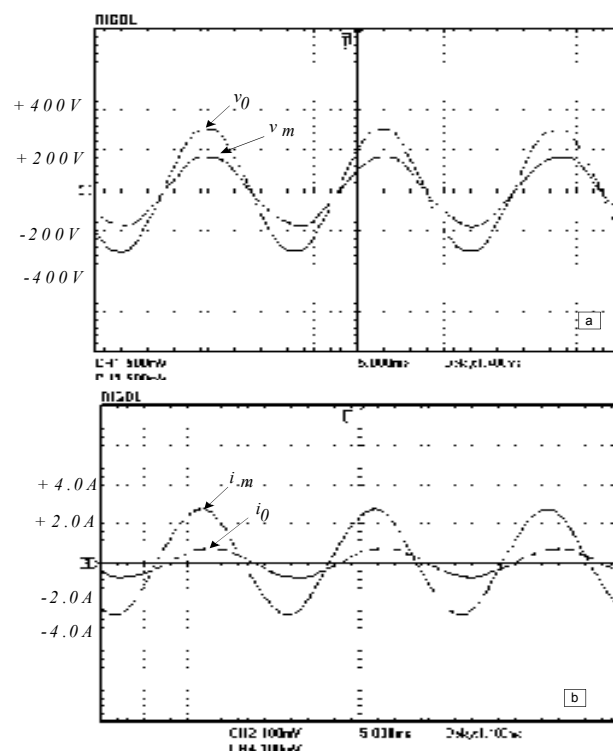


Figure 8. a) Waveforms of the v_o voltage, v_m voltage; b) Waveforms of the i_o current, and i_m current for $D=0.4$

Figure 9(a), 9(b) and Figure 10(a), 10(b) respectively, show the same waveforms for $D=0.48$ and $D=0.56$.

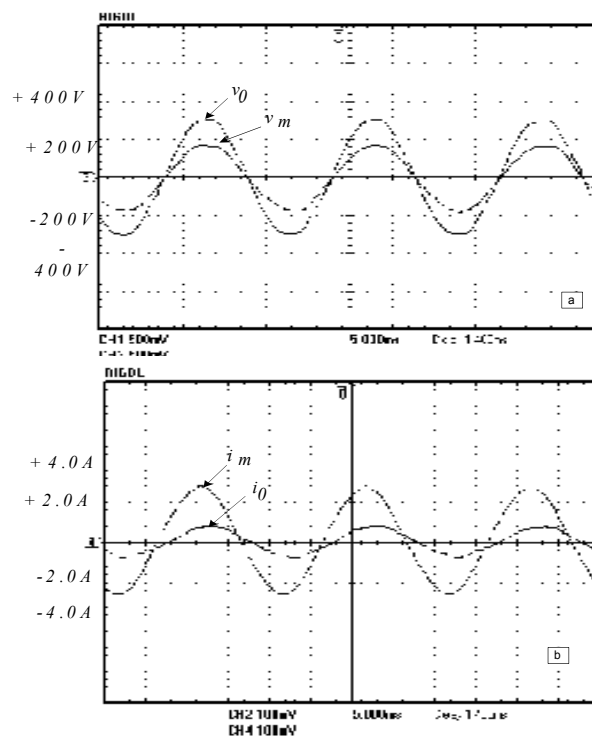


Figure 9. a) Waveforms of the v_o voltage, v_m voltage; b) Waveforms of the i_o current, and i_m current for $D=0.48$

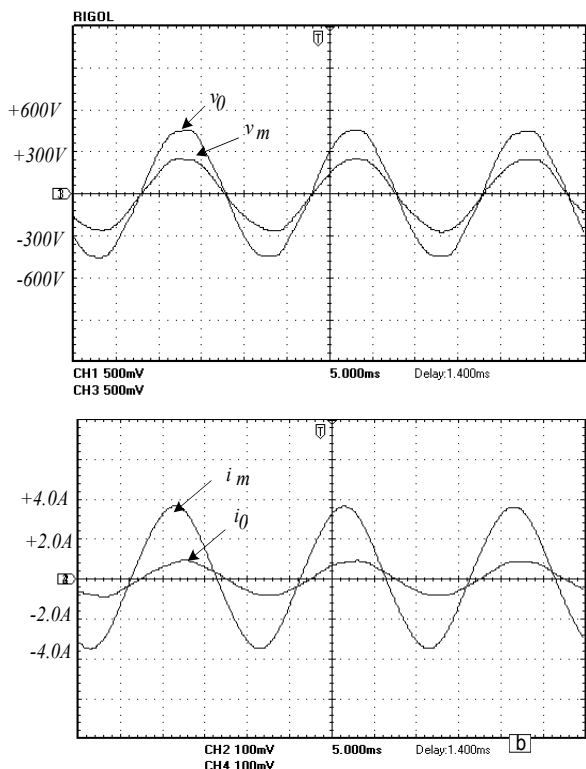


Figure 10. a) Waveforms of the v_o voltage, v_m voltage; b) Waveforms of the i_o current, and i_m current for $D=0.56$

Figure 11 shows the variations of the efficiency depending on the D duty cycle, also based on the simulation results. We notice thus that the efficiency is high for all the values of D .

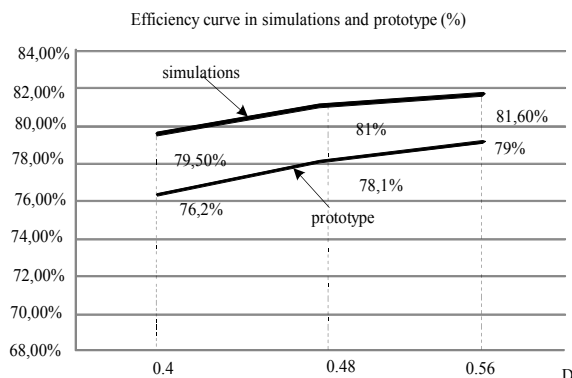


Figure 11 Variation of the efficiency depending on the D duty cycle.

For calculating the THD , total harmonic distortion of the input current, the following equation was used:

$$THD_i = \frac{\sqrt{I_{02}^2 + I_{03}^2 + I_{04}^2}}{I_{01}} \quad (20)$$

where I_{01} is the RMS value of the fundamental input current, I_{02} is the RMS value of the first harmonic of the input current at a switching frequency of 20kHz, etc.

Figure 12 compares (prototype vs. simulation) the THD analyses of the current supplied by the power source.

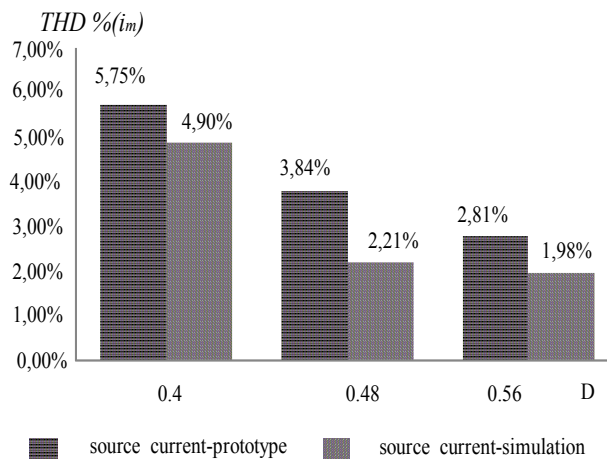


Figure 12. THD analysis for the current supplied by the power source i_m

The input power factor PF can be determined directly from the THD of the input current as follows:

$$PF = \frac{1}{\sqrt{1 + \left(\frac{\%THD_i}{100}\right)^2}} \cos \varphi \quad (20)$$

where φ is the angle between the fundamental component of the input current and the fundamental component of the input voltage.

Figure 13 compares (prototype vs. simulation) the PF analyses of the current supplied power source [21]

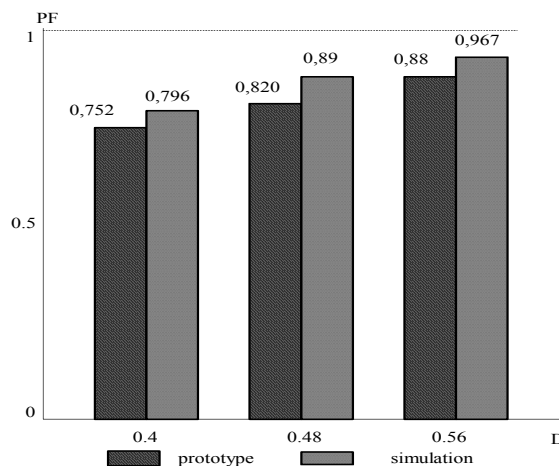


Figure 13. PF analysis for the current power source i_m

IV. CONCLUSION

The paper presents a circuit of direct AC-AC boost converter containing, beside the grid filter, two bidirectional current switches, each made up of one IGBT, four diodes and a boost inductance.

Switches were controlled by uniform sampling, with the same duty cycle in all the switching periods. The resulting control circuit is simple and the energy flow can be bidirectional. The adequate functioning of the circuit was tested by simulation, as well as on a laboratory prototype

The results allowed the identification of the control characteristic and of the functioning efficiencies.

The waveforms obtained for the load voltage and current are very good. The supplied current is sinusoidal, therefore the circuit can be used particularly for converting the RMS voltage from 110V to 220V.

REFERENCES

- [1] G. N. Revenkar, D. S. Trasi, Symmetrical Pulse Width Modulated A. C. Chopper, IEEE Trans. on Ind. Electron. Contr. Instrum., vol.IECI-24, 1977, pp. 41 – 45.
- [2] G. Chose, M. Park, An Improved PWM Technique for A.C. Chopper, IEEE Trans. on Power Electronics, vol 4, 1989, pp. 496 - 505.
- [3] D. Jang, G. Choe, Asymmetrical PWM Method for A.C. Chopper with Improved Input Power Factor, IEEE PESC Conf. Rec, 1991, pp. 838 - 845.
- [4] Jang Do-Hyum, Ghy-Ha Choe, M. Ehsany, Asymmetrical PWM Technique with Harmonic Elimination and Power Factor Control in A.C. Chopper, IEEE Trans. on Power Electron., vol. 10, Nr. 2, March 1995, pp.175-184.
- [5] M. Lucanu, O.Ursaru, C. Aghion, Single Phase A.C. Choppers with I.G.B.T's, Proceedings of the International Symposium on Signal, Circuits and Systems SCS 2003, July 10-11, 2003, pp. 213 - 216.
- [6] L. Congwei, W. Bin, N. R. Zargari, X. Devei, and W. Jiacheng, A novel three-phase three leg AC/AC converter using nine IGBT's, IEEE Trans. on Power Electron., vol. 24, Nr. 5, May 2009, pp. 1151 - 1160.
- [7] R. Lai, F. Wang, R. Burgos, Y. Pei, D. Boroyevich, B.Wang, T. A. Lipo, V. D. Immanuel, K. J. Karimi, A Systematic topology evaluation methodology for high-density three-phase PWM AC-AC converters, IEEE Trans. on Power Electron., vol. 24, Nr. 7, July 2009, pp. 1671 - 1681.
- [8] M. Lucanu, O.Ursaru, C. Aghion, Single Phase A.C. Choppers with Inductive Load and Improved Efficiency, Proceedings of the International Symposium on Signal, Circuits and Systems, ISSCS 2005, vol. 2, July 14-15 2005, pp. 597 - 600.
- [9] J. H. Kim, B. D. Min, B. H. Kwon, S. C. Won, A PWM buck-boost AC chopper solving the commutation problem, IEEE Trans. on Ind. Electron., vol 45, No. 5 1998, pp. 832 - 835.
- [10] L. Li, Y. Yang, Q. Zhong, Novel family of single-stage three level A.C. Choppers, IEEE Trans. on Power Electron., vol. 26, Nr. 2 2001, pp. 504 - 511.
- [11] Thiago B. Soliero, Clovis A. Petry, Joao C. dos S. Fagundes, Yvo Barbi, Direct AC-AC converters using commercial power modules applied to voltage restorers, IEEE Trans. on Ind. Electron., vol 58, No. 1 2011, pp. 278 - 288.
- [12] C. Aghion, M. Lucanu, O.Ursaru, N. Lucanu, Direct AC-AC Step-Down Single-Phase Converter with Improved Performances, Electronics and Electrical Engineering, vol.18, no.10 2012, pp. 33 - 36.
- [13] B. Mammano, B. Carsten, Understanding and optimizing electromagnetic compatibility in switch-mode power supplies, TI power seminar series 2003.
- [14] J. Harper, Electromagnetic compatibility design for power supplies, Fairchild Semiconductor power seminar series 2004/2005
- [15] R. L. Ozenbaugh, EMI filter design , CRC, Nov 2000
- [16] C. Basso, Switch-Mode Power Supplies SPICE Simulations and Practical Designs, McGraw-Hill, 2008
- [17] A. Hesener, Electromagnetic Interference (EMI) in Power Supplies, Fairchild Semiconductor Power Seminar 2010-2011
- [18] Programming languages — C, International Standard, ISO/IEC 9899:TC2
- [19] A. Valachi, M. Timis, M. Danubianu, Some Contributions to Synthesis and Implementation of Multifunctional Registers, 11th WSEAS Int.Conf. on Automatic Control, Modelling & Simulation (acmos'09), Istanbul, Turkey, May 30 - June 1, 2009, p.146-149.
- [20] K. B. Bose, Microcomputer Control of Power Electronics and Drive, IEEE Press. New York, 1987.
- [21] I. V. Pletea, M., Pletea, D., Alexa, N., Lucanu, "Simulations and Analysis and Operating Regime as Rectifier with Power Factor Correction of Two - Quadrant Converter with RNSIC," Advances in Electrical and Computer Engineering, Volume 11, Number 3, Year 2011, pp. 29 – 34.